

# SRRT: Search Region Regulation Tracking

Jiawen Zhu, Xin Chen, Dong Wang\*, Wenda Zhao, Huchuan Lu

School of Information and Communication Engineering, Dalian University of Technology, China  
{jiawen, chenxin3131}@mail.dlut.edu.cn, {wdice, zhaowenda, lhchuan}@dlut.edu.cn

## Abstract

Dominant trackers generate a fixed-size rectangular region based on the previous prediction or initial bounding box as the model input, *i.e.*, search region. While this manner leads to improved tracking efficiency, a fixed-size search region lacks flexibility and is likely to fail in cases, *e.g.*, fast motion and distractor interference. Trackers tend to lose the target object due to the limited search region or be interfered by distractors due to excessive search region. In this work, we propose a novel tracking paradigm, called Search Region Regulation Tracking (SRRT), which applies a proposed search region regulator to estimate an optimal search region dynamically for every frame. To adapt the object’s appearance variation during tracking, we further propose a locking-state determined updating strategy for reference frame updating. Our SRRT framework is very concise without fancy design, yet achieves evident improvements on the baselines and competitive results with other state-of-the-art trackers on seven challenging benchmarks. On the large-scale LaSOT benchmark, our SRRT improves SiamRPN++ and TransT with the absolute gains of 4.6% and 3.1% in terms of AUC.

## 1 Introduction

Given the initial position of arbitrary object, visual object tracking is to predict the target object position accurately and steadily in subsequent sequences. As a fundamental task in computer vision, tracking is widely used in many fields, such as video monitoring (Tian et al. 2011), robotics (Sakagami et al. 2002) and UAV vision (Du et al. 2018). Substantial progress has been achieved, mainly owing to deep feature extracting (Krizhevsky, Sutskever, and Hinton 2012; Szegedy et al. 2015; He et al. 2016; Vaswani et al. 2017), adaptive appearance modeling (Henriques et al. 2008; Danelljan et al. 2019; Bhat et al. 2019, 2020), and correlation matching (Bertinetto et al. 2016; Li et al. 2018; Zhang et al. 2020). Meanwhile, challenges remain, arising from polytropic appearance and motion state, distractor interference, background clutter, *etc.*

Mainstream tracking approaches (Bertinetto et al. 2016; Li et al. 2018, 2019; Danelljan et al. 2019; Bhat et al. 2019; Zhang et al. 2020; Chen et al. 2021; Yan et al. 2021) generate a Region of Interest (ROI) for each frame inference. This region, also named search region, is usually an extended rect-

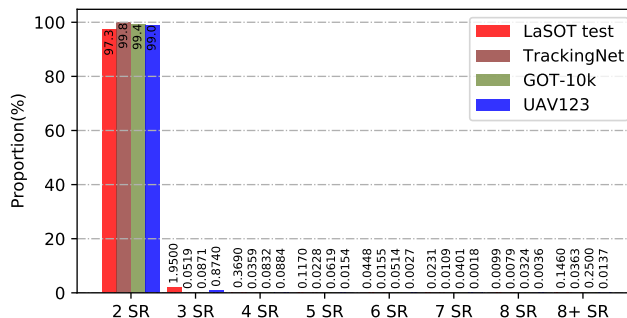


Figure 1: Minimum search region size distribution statistics of adjacent frames. ‘ $N$  SR’: search region of  $N^2$  times of previous object area. Best viewed with zoom-in.

angle region centered on the previous predicted results or initial bounding box. Once acquired, the ROI will be sent to a deep neural network for object locating and scale estimation. A prior condition of obtaining the ROI by this manner is the spatio-temporal continuity (Bennett et al. 2004) of physical objects. Consequently, the previous location of the object can provide an indication of where the network should pay attention to (Held, Thrun, and Savarese 2016). Capturing target object within a search region instead of the whole image greatly improves the efficiency. Widespread, and long-term usage of this strategy, demonstrating its practicality and effectiveness in tracking task.

Regardless of wide applications, the above tracking paradigm’s limitations remain exist. In that paradigm, search region of each frame is obtained by the fixed-size expansion on the previous predicted location. Taking the object movement and tracker’s estimation deviation into account, the expansion is usually several times the estimated target object area (*e.g.*,  $2^2$  times in GOTURN (Held, Thrun, and Savarese 2016),  $4^2$  times in SiamRPN (Li et al. 2018), and  $5^2$  times in KYS (Bhat et al. 2020)). When using a fixed-size search region, trackers are tend to lose the object because of the limited search region, conversely, be interfered by distractors due to excessive range. Particularly, when the tracking fails, the tracker will experience difficulty recovering from drift due to the regional limitations of the fixed-size search region. What size of search region is appropriate for each frame? This problem is worthy of exploration but ignored by researchers.

Fig. 1 shows the minimum search region size distribu-

\*Corresponding Author

tion of adjacent frames on four benchmarks. We utilize the ground truth of the previous frame to calculate the minimum search area size required in the current frame. The statistical results of two adjacent frames show that  $2^2$  times of search region occupies 97.3%, 99.8%, 99.0%, and 99.4% in LaSOT (Fan et al. 2019), TrackingNet (Muller et al. 2018), UAV123 (Mueller, Smith, and Ghanem 2016), and GOT-10k (Huang, Zhao, and Huang 2019), respectively. This finding indicates that a tracker can sufficiently capture the target object in the next frame with a small size search region in most time. Meanwhile, in some cases, extraordinary large search region is required, such as  $8^2$  times larger than the target object in previous frame. Although those cases is rare, neglecting them will result in a broken of trajectory chain. In this paper, we propose a novel tracking paradigm, called Search Region Regulation Tracking (SRRT), which can generate dynamic search region for tracking. Compared with conventional paradigm (shown in Fig. 2 (a)), SRRT (shown in Fig. 2 (b)) applies a search region regulator (SRR) to allocate an optimal search region. Benefiting from the advance perception of ROI, SRRT tracks a target object with a small size search region most of the time, and can flexibly switch to a larger search radius when encountering the case such as fast motion. In addition, the variation of the object appearance during online tracking usually obscures the reference information of the initial frame. We further propose a locking-state determined reference frame updating strategy to improve robustness to search region awareness. More importantly, our SRRT can be easily applied to existing trackers. In summary, the main contributions are as follows:

- We propose SRRT, a novel Search Region Regulation Tracking paradigm. Instead of choosing a fixed-size search region in all scenarios, SRRT explores dynamically selecting an optimal search region for each frame, delivers higher performance while being efficient.
- We propose a locking-state determined update strategy to improve the richness of reference information to adapt to the challenges caused by the variation of object appearance.
- Extensive experiments on seven widely used benchmarks demonstrate the effectiveness of the proposed method. SRRT can be easily applied to existing trackers, brings consistently improvements on baselines and achieves state-of-the-art performance.

## Search Region Generation

The mainstream tracking paradigm usually extends a search region centered on previous prediction location for the current frame tracking, which is based on prior information, that is, the location and scale changemement of the target object in the consecutive sequence are continuous. SiamFC (Bertinetto et al. 2016) adds margin to object bounding box to generate search region with a size of  $255 \times 255$  pixels, approximately  $4^2$  times larger than the target object area. GOTURN (Held, Thrun, and Savarese 2016) proposes to adopt a 0 mean Laplace distribution to model smoothness of object motion and scale changes through space. The search radius is twice the width and height

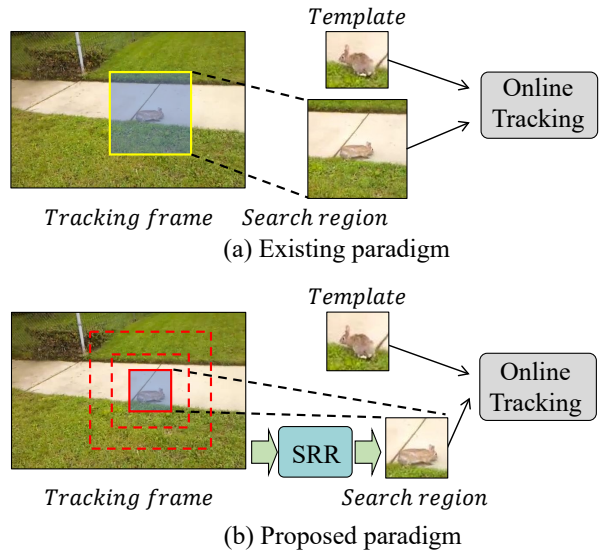


Figure 2: Paradigm of existing approaches (a) and ours (b).

of the predicted bounding box in the previous frame. The tracker can better adapt to small movements, thereby achieving the continuity of tracking. To exploit scene information, KYS (Bhat et al. 2020) applies a  $5^2$  times search region as large as the shape of the target object and combines the propagated dense localized vectors with the appearance model features to localize the target object. Due to the introduction of more sufficient information in spatial and temporal dimensions, KYS utilizes an extra propagation module and online status update. SiamR-CNN (Voigtlaender et al. 2020) is more robust to tracking drift by explicitly modeling the motion and interactions of all potential objects. Despite obtaining excellent performance, it is extremely slow because it feeds the full-size image into the tracking network. Most of the other trackers also use a fixed search region for target object capturing, *e.g.*  $4^2$  times (Li et al. 2018; Wang et al. 2019; Zhang et al. 2020) and  $5^2$  times (Danelljan et al. 2019; Bhat et al. 2019) the size of previous object shape.

These methods employ different search regions, from  $2^2$  times as large as target object area to the whole image. A small search region brings advantages in speed, but it can easily lose the target object, *e.g.*, when the target object moves quickly. A large search region increases the search scope, but it also needs to face the increased distractors. Therefore, a complex identity discrimination or association module needs to be designed to filter the interference. To deal with occlusion in long-term tracking, tracking-learning-detection (TLD) method (Kalal, Mikolajczyk, and Matas 2012) combines a local tracker and a global re-detector. On the contrary, our work implements a more concise and flexible online tracking paradigm, which predicts an optimal search region for each frame, improving performance while being concise.

## 2 Search Region Regulation Tracking

In this section, we describe how our method (Fig. 3) achieves online tracking with a regulated search region. We ini-

tially revisit the standard search region generation approach and analyze its limitations. Subsequently, we introduce the formulation of our search region regulation and describe the components and training process of our model in detail. Last, the pipeline of SRRT framework is described.

### Conventional Search Region Generation

Existing trackers (Held, Thrun, and Savarese 2016; Li et al. 2018; Danelljan et al. 2019) generate a ROI for appearance modeling of each frame. This manner is based on accuracy in the previous prediction of the tracker. Because it is simple and effective, this manner has dominated tracking until now. For one particular target object, most trackers exploit its location  $\mathbf{L}_{t-1} : (c_x^{t-1}, c_y^{t-1})$  and scale  $\mathbf{S}_{t-1} : (h^{t-1}, w^{t-1})$  in the  $(t-1)$ th frame, and directly yield the search region  $\mathbf{X}_t \in \mathbb{R}^{m_R \times n_R \times 3}$  for current frame tracking,

$$\mathbf{X}_t = \text{crop}(\mathbf{L}_{t-1}, \gamma \mathbf{S}_{t-1}), \quad (1)$$

where  $\text{crop}(\cdot)$  represents cropping the region centered on  $\mathbf{L}_{t-1}$  to generate the corresponding search region. The search radius factor  $\gamma$  is set to a fixed value (e.g.,  $\gamma = 4$ ). Tracker performs appearance modeling and matching in this region that is  $\gamma^2$  times the previous target object area.

In this work, we argue that this hidebound manner limits tracker’s performance. Its limitations mainly include the following: **(i)** applying fixed search region for every video, every frame, can barely aware the existence of the target object, which means trackers may lose the target object caused by some factors, e.g., fast motion, or be interfered by distractors due to excessive search region range. **(ii)** Once tracking fails, the tracker lacks adaptability, suffering from difficulty to rediscover the target object due to limited search region. **(iii)** In order to alleviate the phenomenon of target object losing, most trackers adopt a larger search region, which may reduce the efficiency of online tracking.

### Learning Search Region Regulation

How is an appropriate search region for frame-level tracking obtained? We propose to estimate a proper search region dynamically. The essential part in SRR is to estimate the search radius factor  $\tilde{\gamma}_t \in \{\tilde{\gamma}_j\}_{j=1}^M$  for each frame through given information according to,

$$\tilde{\gamma}_t = \text{Argmax}(\mathcal{F}_{SRR}(\mathbf{Z}_0, \mathbf{C}_t)), \quad (2)$$

where  $\mathcal{F}_{SRR}(\cdot)$  donates the learned generic function for search region regulation.  $\mathbf{Z}_0 \in \mathbb{R}^{m_0 \times n_0 \times 3}$  represents target reference patches, and  $\mathbf{C}_t \in \mathbb{R}^{m_c \times n_c \times 3}$  represents the candidate region patches of the current frame for search region regulation function. Specifically, candidate region  $\mathbf{C}_t$  is similar to search region but only used by SRR. The learned function  $\mathcal{F}_{SRR}(\cdot)$  computes the probability for search radius factor  $\tilde{\gamma}_j$  by using the reference target  $\mathbf{Z}_0$  and the candidate region  $\mathbf{C}_t$  patches. In addition,  $\text{Argmax}(\cdot)$  denotes the optimal search radius factor  $\tilde{\gamma}_t$ . Figuratively,  $\mathcal{F}_{SRR}(\cdot)$  attempts to simulate the human behavior when tracking a target object, that we firstly glance to determine its approximate location before finding its extract position. Therefore, the tracker can obtain an optimal search region in frame-level, improving the adaptability for variable target movement states. In

this work,  $\mathcal{F}_{SRR}(\cdot)$  is implemented as a neural network, which can learn general mapping by large amount of data. Moreover, search region regulation is independent of subsequent tracking process; it does not affect the tracker’s feature representation for localization and scale estimation. Thus, they can be flexibly integrated into existing trackers.

### Search Region Regulator

**Model Design.** We present the structure of our search region regulation module in Fig. 3. The pipeline is described in an online tracking process. The entire SRR  $\mathcal{F}_{SRR}(\cdot)$  is extremely simple; it employs a siamese-based architecture to match the reference target object from the candidate region. We adopt dual reference patches, an initial reference  $\mathbf{Z}_0$  sampling from ground-truth bounding box in the initial frame, and a dynamic reference  $\mathbf{Z}_d \in \mathbb{R}^{m_d \times n_d \times 3}$  updating by online tracking results. These two patches are used for robust search region regulation on a candidate region  $\mathbf{C}_t$ , which is  $6^2$  times of search region. A ResNet-50 (He et al. 2016) backbone is employed for feature extracting from reference and candidate region patches. Reference features ( $\mathbf{f}_0, \mathbf{f}_d$ ) and candidate features  $\mathbf{f}_c$  are correlated by the depth-wise correlation operation (Wang et al. 2019; Li et al. 2019). The correlated features is firstly sent to a parameter-sharing convolution block. The produced two feature maps are concatenated and then sent to a  $1 \times 1$  convolutional layer used as weighted summation. Lastly, a prediction head consisting of a three-layer MLP outputs the probability  $\mathbf{P}_t$  for different search radius factors. The search region regulation with a dynamic reference can be described as follows:

$$\tilde{\gamma}_t = \text{Argmax}(\mathcal{F}_{SRR}(\mathbf{Z}_0, \mathbf{Z}_d, \mathbf{C}_t)), \quad (3)$$

Compared with the general siamese tracker, the feature interaction part of our search region regulator is very lightweight and simple, because the tracker network needs to complete accurate target object locating, whereas the search region regulator only needs to predict the category of the search region.

**Locking-state Determined Update.** Dynamic reference frame is beneficial to improve the adaptation to target’s appearance change during online tracking. Some existing approaches (Yan et al. 2021; Borsuk et al. 2021) also use a dual-template representation for target model adaptation. Different from these approaches, we propose a locking-state determined update strategy which does not require any extra network or metrics to be used as update judgments. On the contrary, as shown in Fig. 3, we record the search region selected for each frame in a sequence. When the SRRT selects the smallest search region for consecutive frames, we name this situation as target-locking. Once this situation appears, the model updates the dynamic reference  $\mathbf{Z}_d$  with  $\mathbf{Z}'_d$  from the current frame. Another thing to note is that our locking-state determined update strategy is designed for the SRR, not the base tracker, so our SRR module is completely independent of the SR-dedicate base trackers.

**Training Approach.** For training our search region regulator, we randomly sample three frames in the same video sequence with an interval of no more than 100 frames to generate the reference and candidate region patches. The initial

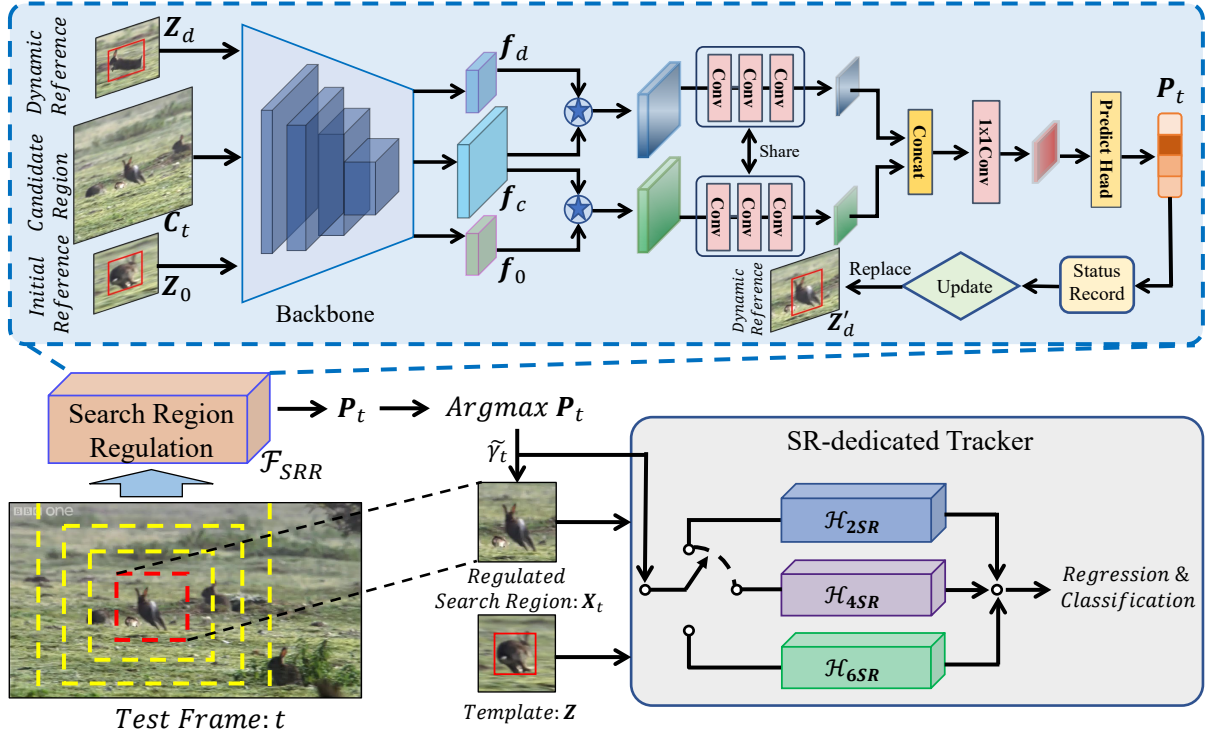


Figure 3: Overview of our SRRT paradigm.

reference frame and candidate region are always from the beginning or end of a sequence. Two reference patches and one candidate region form a sampling pair. The candidate patches are sampled with different search region distributions for model training. The location  $L : \{c_x, c_y\}$  and scale  $S : \{h, w\}$  of sampling candidate region are determined by the following equations:

$$\{h, w\} = \{h_{gt}, w_{gt}\} \times \gamma_{train} \times e^{\delta_S}, \quad (4)$$

$$\{c_x, c_y\} = \{c_x^{gt}, c_y^{gt}\} + \frac{h+w}{2} \times \delta_C, \quad (5)$$

where,  $h_{gt}, w_{gt}, c_x^{gt}$ , and  $c_y^{gt}$  are obtained from the ground-truth bounding box, and we set search radius  $\gamma_{train} = 6$ .  $\delta_S$  and  $\delta_C$  are factors for scale and location jitters as data augmentation. Specially, we apply variable  $\delta_C$  to form the sample pairs with different categories of search region. The training set  $T = \{(C_i, Z_0^i, Z_d^i, Y_i)\}_{i=1}^n$  consists of three input patches and search region category annotation  $Y_i$ . In our experiments, the sampling ratio of search region categories are set to  $2SR : 4SR : 6SR : 8SR = 1 : 1 : 1 : 1$ ;  $8SR$  samples are used to simulate the situation that the target object is not in the candidate region. The reference and candidate region are resized to  $384 \times 384$  and  $128 \times 128$  pixels, respectively. The search region regulator network merely uses a cross-entropy loss  $L_c$ , as follows:

$$L_c = -\frac{1}{N} \sum_{i=1}^N \sum_{j=1}^M y_{i,j} \log(p_{i,j}) \quad (6)$$

where  $M$  denotes the number of search region categories, and  $N$  is size of a mini-batch.  $y_{i,j}$  and  $p_{i,j}$  represent

the ground-truth and predicted probability for  $j$ th category search region of  $i$ th sample.

### SRRT Framework

In this subsection, we describe the pipeline of SRRT framework for online tracking. As shown in Fig. 3, reference patches ( $Z_0, Z_d$ ) and candidate region patches  $C_t$  are sent to the search region regulation module, and an optimal search radius factor  $\tilde{\gamma}_t$  is predicted by search region regulator. Then, the search region patch is cropped in terms of  $\tilde{\gamma}_t$ . In order to handle search regions with different search radius, SR-dedicated trackers are trained. We employ three SR-dedicated trackers  $\mathcal{H}_{2SR}$ ,  $\mathcal{H}_{4SR}$ , and  $\mathcal{H}_{6SR}$ , which are  $2^2$ ,  $4^2$ , and  $6^2$  times of the target area, respectively. Specially,  $\mathcal{H}_{6SR}$  is employed for handling search regions equal or larger than  $6^2$  times of the target area. The corresponding SR-dedicated tracker is selected in terms of  $\tilde{\gamma}_t$  for the current frame online tracking. Lastly, the regression and classification results are output. SRRT paradigm flexibly provides suitable search regions for different tracking scenarios and combines the power of different SR-dedicated trackers through online dynamic switching.

## 3 Experiments

### Implementation Details

Our algorithm is implemented with the Pytorch (Paszke et al. 2017) library. We verify the effectiveness of SRRT on seven benchmarks, including LaSOT (Fan et al. 2019), TrackingNet (Muller et al. 2018), GOT-10k (Huang, Zhao, and Huang 2019), UAV (Mueller, Smith, and Ghanem

Table 1: State-of-the-art comparison on LaSOT (Fan et al. 2019), TrackingNet (Muller et al. 2018), GOT-10k (Huang, Zhao, and Huang 2019), UAV123 (Mueller, Smith, and Ghanem 2016), and LaSOT<sub>ext</sub> (Fan et al. 2021) test benchmarks. \* denotes the results provided by us, and the SRRSiamRPN++ is based on SiamRPN++\*. The best two result are in **bold** fonts. Our methods achieves competitive results compared with other state-of-the-art trackers.

Methods	LaSOT			TrackingNet			GOT-10k			UAV123		LaSOT <sub>ext</sub>		
	AUC	P <sub>Norm</sub>	P	AUC	P <sub>Norm</sub>	P	AO	SR <sub>50</sub>	SR <sub>75</sub>	AUC	P	AUC	P <sub>Norm</sub>	P
SiamFC	33.6	42.0	33.9	57.1	66.3	53.3	34.8	35.3	9.8	48.5	69.3	23.0	31.1	26.9
MDNet	39.7	46.0	37.3	60.6	70.5	56.5	29.9	30.3	9.9	52.8	-	27.9	34.9	31.8
ECO	32.4	33.8	30.1	55.4	61.8	49.2	31.6	30.9	11.1	52.5	74.1	22.0	25.2	24.0
SiamRPN++	49.6	56.9	49.1	73.3	80.0	69.4	51.7	61.6	32.5	61.0	80.3	34.0	41.6	39.6
ATOM	51.5	57.6	50.5	70.3	77.1	64.8	55.6	63.4	40.2	64.3	-	37.6	45.9	43.0
DiMP	56.9	65.0	56.7	74.0	80.1	68.7	61.1	71.7	49.2	65.4	-	39.2	47.6	45.1
SiamFC++	54.4	62.3	54.7	75.4	80.0	70.5	59.5	69.5	47.9	-	-	-	-	-
OCEAN	56.0	65.1	56.6	-	-	-	61.1	72.1	47.3	-	-	-	-	-
PrDiMP	59.8	68.8	60.8	75.8	81.6	70.4	63.4	73.8	54.3	68.0	-	-	-	-
SiamR-CNN	64.8	72.2	-	81.2	85.4	80.0	64.9	72.8	59.7	64.9	<b>83.4</b>	-	-	-
STMTracker	60.6	69.3	63.3	80.3	85.1	76.7	64.2	73.7	57.5	64.7	-	-	-	-
TrDiMP	63.9	-	61.4	78.4	83.3	73.1	67.1	77.7	58.3	67.5	-	-	-	-
STARK	67.1	<b>77.0</b>	-	<b>82.0</b>	<b>86.9</b>	-	68.8	78.1	64.1	-	-	-	-	-
KeepTrack	<b>67.1</b>	<b>77.2</b>	<b>70.2</b>	-	-	-	-	-	-	<b>69.7</b>	-	<b>48.2</b>	-	-
SiamRPN++*	52.3	59.1	52.4	75.1	80.5	71.0	57.6	66.6	46.5	62.1	78.5	35.4	40.0	38.1
TransT	64.9	73.8	69.0	81.4	86.7	<b>80.3</b>	<b>72.3</b>	<b>82.4</b>	<b>68.2</b>	69.1	-	45.1	<b>51.3</b>	<b>51.2</b>
<b>SRRSiamRPN++</b>	56.9	64.0	57.1	76.0	81.3	71.9	58.4	67.8	47.9	62.8	78.8	37.0	41.7	40.0
<b>SRRTransT</b>	<b>68.0</b>	76.9	<b>72.4</b>	<b>82.1</b>	<b>87.2</b>	<b>80.4</b>	<b>72.2</b>	<b>81.8</b>	<b>67.2</b>	<b>71.1</b>	<b>88.5</b>	<b>47.4</b>	<b>54.0</b>	<b>54.1</b>

2016), LaSOT<sub>ext</sub> (Fan et al. 2021), NFS (Kiani Galoogahi et al. 2017), and OTB100 (Wu, Lim, and Yang 2015). We take two classic trackers, SiamRPN++ (Li et al. 2019) and TransT (Chen et al. 2021) as our base tracker. SiamRPN++ (Li et al. 2019) is a representative work of the saimese-based methods, and TransT (Chen et al. 2021) is a recent transformer-based method.

**Offline Training.** The training set of our SRR module includes the training splits of LaSOT (Fan et al. 2019), GOT-10k (Huang, Zhao, and Huang 2019), COCO (Lin et al. 2014), and TrackingNet (Muller et al. 2018). The reference patches are resized to 128×128 pixels, and the candidate patches are resized to 384×384 pixels. The SRR module employs a ResNet-50 (He et al. 2016) backbone initialized with ImageNet (Russakovsky et al. 2015) pretrained parameters. AdamW (Loshchilov and Hutter 2018) optimizer is adopted during model training. The learning rate is set to 1e-3 and decayed by 10× at every 30 epochs; And the weight decay is 1e-4. The SRR model is trained on two Nvidia RTX 2080Ti GPUs for 90 epochs with a batch size of 32. Each epoch includes 50,000 sample pairs.

For SR-dedicated base tracker, we trained two other TransT (Chen et al. 2021) models that adopted 2<sup>2</sup> times and 6<sup>2</sup> times search region. We use the original TransT parameters as our 4<sup>2</sup> times search region model. The template patches are resized to 128×128 pixels, and the search regions of 2<sup>2</sup>, 4<sup>2</sup>, 6<sup>2</sup> times are resized to 128×128,

256×256, and 384×384 pixels, respectively. The other training settings for different search regions are consistent with the original version. For the convenience of experiments, SimaRPN++(Li et al. 2019) was reproduced with different search regions. The model architecture is maintained the same as that in the original paper except for training datasets and optimizer. We use the same training datasets and optimizer as the TransT model.

**Online Tracking.** During inference, only window penalty is applied; it is also used in SiamRPN++(Li et al. 2019) and TransT (Chen et al. 2021) to reweigh the classification score maps. In addition, our SRRT framework does not have any online fine-tuning modules.

### State-of-the-art Comparison

**LaSOT.** LaSOT (Fan et al. 2019) is a large-scale single-object tracking benchmark, which consists of 1400 sequences. It contains many long sequences and challenging scenes of distractors. The results in terms of success (AUC), normalized precision (P<sub>Norm</sub>), and precision (P) are shown in Tab. 1.

Our SRRSiamRPN++ outperforms SiamRPN++ with a large margin, 4.6% and 4.9% on AUC and P<sub>Norm</sub>, respectively. These improvements clearly show the benefits of regulating an adaptive search region for open-world scene tracking. SRRTransT outperforms the current state-of-the-art trackers, e.g., STARK (Yan et al. 2021) and Keep-

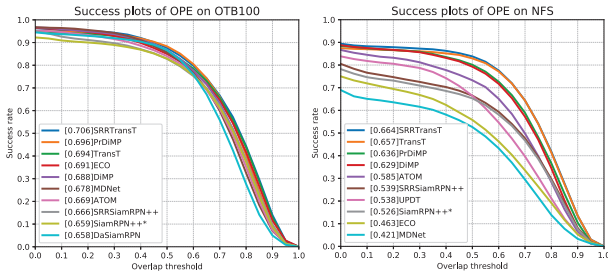


Figure 4: State-of-the-art comparison on OTB100 and NFS. Best viewed with zoom-in.

Track (Mayer et al. 2021), even though TransT has a gap between them.

**TrackingNet.** TrackingNet (Muller et al. 2018) is a large-scale tracking dataset containing rich distributions of object classes. The performance evaluation is provided on an online official server following the one-pass evaluation protocol. Tab. 1 shows the AUC,  $P_{Norm}$ , and P results. Our SRRTransT achieves the best performance, namely, 82.1%, 87.2%, and 80.4% for AUC,  $P_{Norm}$ , and P, respectively. Our SRRT paradigm boosts TransT and SiamRPN++ consistently, increasing AUC from 81.4% and 75.1% to 82.1% and 76.0%.

**GOT-10K.** GOT-10k (Huang, Zhao, and Huang 2019) is a tracking dataset that broadly covers 560 classes of common outdoor moving objects. We submit results to its online evaluation server. Average overlap (AO) is employed for performance measure. As shown in Tab. 1, SRRTransT achieves AO of 72.2%, which is a very similar performance to the baseline. For SRRSiamRPN++, the AO score increases to 58.4%. The results show that our SRRT can generalize effectively on different scenarios and challenges.

**UAV123.** UAV123 (Mueller, Smith, and Ghanem 2016) contains 123 low-altitude aerial videos with 9 object categories. Similar to LaSOT (Fan et al. 2019), it contains long sequences and distractor scenes, which can be challenging for robust object tracking. As shown in Tab. 1, SRRT boosts the performance of the baselines. SRRTransT achieves the state-of-the-art performance with the AUC of 71.1%.

**LaSOT<sub>ext</sub>.** LaSOT<sub>ext</sub> is an extension dataset of LaSOT, containing 150 videos of 15 object categories, which is more challenge than LaSOT. As shown in Tab. 1, SRRTransT and SRRSiamRPN++ outperform their baselines by 2.3% and 1.6% in terms of AUC, respectively. Our SRRTransT achieves a competitive AUC (47.4%) with the current best method KeepTracker (Mayer et al. 2021) while has a  $2\times$  faster (41.8 vs 18.3 *fps*) speed.

**OTB100 and NFS.** OTB100 (Wu, Lim, and Yang 2015) and NFS (Kiani Galoogahi et al. 2017) are two commonly used small-scale benchmarks both including 100 videos. We report the success plots over all videos, and the results are shown in Fig. 4. On OTB100, our SRRTransT obtains the best AUC score of 70.6%, outperforming the previous best method PrDiMP by 1%. SRRTransT and SRRSiamRPN boosting their baselines by a relative gain of 1.7% and 1.1%. On NFS, SRRTransT and SRRSiamRPN achieves 66.4% and 53.9% of AUC score, which outperform the baselines

relatively by 1.1% and 2.5%.

## Ablation Studies

In this subsection, we study our SRRT with TransT (Chen et al. 2021) as the base SR-dedicated tracker, and large-scale benchmark LaSOT (Fan et al. 2019) test set is used for evaluation.

**Component-wise Analysis.** The component-wise study results are shown in Tab. 2. #NUM ① is the original TransT and #NUM ③ is our SRRTransT. In #NUM ②, after applying the search region regulation, the tracker achieves 3.4%, 2.8%, and 3.5% relative improvement on AUC,  $P_{Norm}$ , and P, respectively. This improvement proves the effectiveness of the search region regulation paradigm because it can select a suitable search region flexibility during online tracking. Moreover, we apply the locking-state determined update (LDU) strategy for dynamic reference input. As shown in #NUM ③ of Tab. 2, with dynamic reference updating, the accuracy of the search region regulator are further improved. The AUC,  $P_{Norm}$ , and P are boosted to 68.0%, 76.9%, and 72.4%, respectively, achieving the level of state-of-the-art performance.

**Different size of search region.** To balance the search region requirements in different scenarios, existing trackers usually apply a mezzo fixed-size search region. Therefore, the selected search region is inevitably large or small in some scenarios. As shown in Tab. 3, 4SR obtains better performance than 2SR, and a similar performance to 6SR. When applying a fixed search region, 4SR may be optimal. However, SRRT combines the advantages of each category of search region, delivering more advanced performance than any others. More results are provided in the supplementary material.

**Why SRRT Works?** To analyze how our SRRT framework works, we visualiz several representative tracking clips during online tracking. As shown in Fig. 5, benefiting from dynamic search region switching, SRRT runs smoothly with the smallest search region most of the time (more result can be found in the supplementary material), except when the search radius needs to be increased to prevent the target object from being lost. SRRT applies a small search region in some scenarios, *e.g.* target object has little movement which improves efficiency and avoids distractors (see the first two rows in Fig. 5). SRRT applies a large search region in some scenarios, *e.g.*, losing the target object, which can relocate the target position more precisely when the target object is lost (see the last two rows in Fig 5). SRRT strives for an ideal tracking paradigm, that is, the tracker uses a narrow search region for stably tracking in most of the time; when the target object is likely to be lost, the tracker can widen the search radius to relocate the target object.

**Different Backbones.** As shown in Tab. 4, we investigate the SRR module with different backbones. The ResNet-50 version achieves the best performance with deeper network layers and still has a speed of 41.8 *fps*. When employing the ResNet-18 backbone, the runing speed (47.2 *fps*) almost catches up with the speed of the original TransT (47.3 *fps*), yet 3.4% relatively higher than that of AUC. SRRT has little impact on speed because it selects a small search region

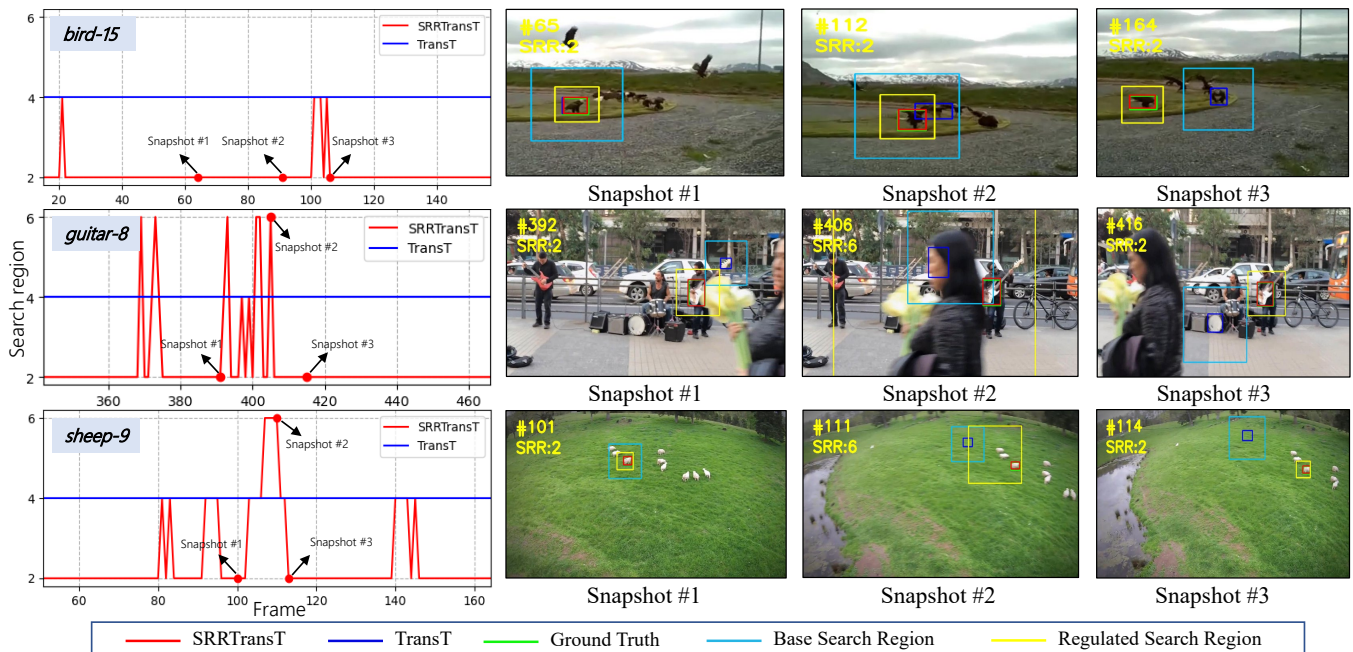


Figure 5: Representative cases with our SRRT scheme. Best viewed in color with zoom-in.

#NUM	Base	SRR	LDU	AUC	$P_{Norm}$	P
①	✓			64.9	73.8	69.0
②	✓	✓		67.1	75.9	71.4
③	✓	✓	✓	68.0	76.9	72.4

Table 2: Component-wise analysis of the proposed model. AUC,  $P_{Norm}$ , and P results demonstrate the importance of each component in our framework.

Method	AUC	$P_{Norm}$	P	Speed	Latency
2SR	59.1	66.7	62.1	51.9	19.3ms
2SR/4SR	65.1	73.7	69.2	42.5	23.5ms
4SR	64.9	73.8	69.0	47.3	21.1ms
4SR/6SR	67.3	76.6	71.6	36.8	27.2ms
6SR	64.6	74.1	67.6	26.9	37.2ms
SRRT	68.0	76.9	72.4	41.8	23.9ms

Table 3: Performance and speed comparison of different categories of search region.

for the main tracking scenes. Moreover, when we directly use a backbone of 5 convolutional layers (the first 5 layers in ResNet-18), the AUC also raises to 66.3%, with a faster speed (49.3 *fps*) than the baseline; it clearly demonstrates the validity of the SRRT paradigm.

**Speed Influence.** We study the speed influence of different search regions and our SRRT paradigm in Tab. 3. Experiments are run on a single Nvidia RTX 2080Ti GPU. With the  $2^2$  times,  $4^2$  times, and  $6^2$  times search region, the base tracker has the speed of 51.9, 47.3 and 26.9 *fps*,

respectively. The latency begins to increase when employing a large search region (6SR). 2SR/4SR and 4SR/6SR means that the search region is restricted to 2SR/4SR and 4SR/6SR, respectively, when running our SRRT. SRRT runs at a real time speed on GPU and outperforms all other solutions in performance.

Method	AUC	$P_{Norm}$	P	Speed	Latency
Base	64.9	73.8	69.0	47.3	21.1ms
+ SRR(Conv-5)	66.3	75.5	70.7	49.3	20.3ms
+ SRR(ResNet-18)	67.1	76.1	71.4	47.2	21.2ms
+ SRR(ResNet-34)	67.5	76.5	71.8	44.6	22.4ms
+ SRR(ResNet-50)	68.0	76.9	72.4	41.8	23.9ms

Table 4: Comparison of SRRT with different backbones.

## 4 Conclusion

This paper proposes a novel tracking paradigm for visual object tracking. Our SRRT achieves accuracy and efficient tracking performance by applying a search region regulator for dynamically selecting an optimal search region size during online tracking. SRRT paradigm alleviates the difficulties in some intractable situations, *e.g.*, target object losing and distractor interference. The framework is simple yet effectively improves the tracking performance remarkably. SRRT significantly boosts baselines on multiple tracking benchmarks, and extensive experiments demonstrate its effectiveness.

## References

- Bennett, B.; Magee, D. R.; Cohn, A. G.; and Hogg, D. C. 2004. Using spatio-temporal continuity constraints to enhance visual tracking of moving objects. In *ECAI 2004 Proceedings of the 16th European Conference on Artificial Intelligence, August 22-27, 2004*, 922–926. IOS Press.
- Bertinetto, L.; Valmadre, J.; Henriques, J. F.; Vedaldi, A.; and Torr, P. H. S. 2016. Fully-Convolutional Siamese Networks for Object Tracking. In *ECCVW*.
- Bhat, G.; Danelljan, M.; Gool, L. V.; and Timofte, R. 2019. Learning Discriminative Model Prediction for Tracking. In *ICCV*.
- Bhat, G.; Danelljan, M.; Gool, L. V.; and Timofte, R. 2020. Know Your Surroundings: Exploiting Scene Information for Object Tracking. In *ECCV*.
- Borsuk, V.; Vei, R.; Kupyn, O.; Martyniuk, T.; Krashenyi, I.; and Matas, J. 2021. FEAR: Fast, Efficient, Accurate and Robust Visual Tracker. *arXiv preprint arXiv:2112.07957*.
- Chen, X.; Yan, B.; Zhu, J.; Wang, D.; Yang, X.; and Lu, H. 2021. Transformer Tracking. In *CVPR*.
- Danelljan, M.; Bhat, G.; Khan, F. S.; and Felsberg, M. 2019. ATOM: Accurate Tracking by Overlap Maximization. In *CVPR*.
- Du, D.; Qi, Y.; Yu, H.; Yang, Y.; Duan, K.; Li, G.; Zhang, W.; Huang, Q.; and Tian, Q. 2018. The unmanned aerial vehicle benchmark: Object detection and tracking. In *Proceedings of the European conference on computer vision (ECCV)*, 370–386.
- Fan, H.; Bai, H.; Lin, L.; Yang, F.; Chu, P.; Deng, G.; Yu, S.; Huang, M.; Liu, J.; Xu, Y.; et al. 2021. Lasot: A high-quality large-scale single object tracking benchmark. *International Journal of Computer Vision*, 129(2): 439–461.
- Fan, H.; Lin, L.; Yang, F.; Chu, P.; Deng, G.; Yu, S.; Bai, H.; Xu, Y.; Liao, C.; and Ling, H. 2019. LaSOT: A High-Quality Benchmark for Large-Scale Single Object Tracking. In *CVPR*.
- He, K.; Zhang, X.; Ren, S.; and Sun, J. 2016. Deep Residual Learning for Image Recognition. In *CVPR*.
- Held, D.; Thrun, S.; and Savarese, S. 2016. Learning to Track at 100 FPS with Deep Regression Networks. In *ECCV*.
- Henriques, J. F.; Caseiro, R.; Martins, P.; and Batista, J. 2008. High-Speed Tracking with Kernelized Correlation Filters. In *ICVS*.
- Huang, L.; Zhao, X.; and Huang, K. 2019. Got-10k: A large high-diversity benchmark for generic object tracking in the wild. *TPAMI*.
- Kalal, Z.; Mikolajczyk, K.; and Matas, J. 2012. Tracking-Learning-Detection. *IEEE Transactions on Pattern Analysis and Machine Intelligence*, 34(7): 1409–1422.
- Kiani Galoogahi, H.; Fagg, A.; Huang, C.; Ramanan, D.; and Lucey, S. 2017. Need for speed: A benchmark for higher frame rate object tracking. In *ICCV*.
- Krizhevsky, A.; Sutskever, I.; and Hinton, G. E. 2012. Imagenet classification with deep convolutional neural networks. In *NIPS*.
- Li, B.; Wu, W.; Wang, Q.; Zhang, F.; Xing, J.; and Yan, J. 2019. SiamRPN++: Evolution of Siamese Visual Tracking with Very Deep Networks. In *CVPR*.
- Li, B.; Yan, J.; Wu, W.; Zhu, Z.; and Hu, X. 2018. High Performance Visual Tracking With Siamese Region Proposal Network. In *CVPR*.
- Lin, T.-Y.; Maire, M.; Belongie, S. J.; Bourdev, L. D.; Girshick, R. B.; Hays, J.; Perona, P.; Ramanan, D.; Dollár, P.; and Zitnick, C. L. 2014. Microsoft COCO: Common Objects in Context. In *ECCV*.
- Loshchilov, I.; and Hutter, F. 2018. Decoupled Weight Decay Regularization. In *ICLR*.
- Mayer, C.; Danelljan, M.; Paudel, D. P.; and Van Gool, L. 2021. Learning target candidate association to keep track of what not to track. In *Proceedings of the IEEE/CVF International Conference on Computer Vision*, 13444–13454.
- Mueller, M.; Smith, N.; and Ghanem, B. 2016. A benchmark and simulator for UAV tracking. In *ECCV*.
- Muller, M.; Bibi, A.; Giancola, S.; Alsubaihi, S.; and Ghanem, B. 2018. TrackingNet: A large-scale dataset and benchmark for object tracking in the wild. In *ECCV*.
- Paszke, A.; Gross, S.; Chintala, S.; Chanan, G.; Yang, E.; DeVito, Z.; Lin, Z.; Desmaison, A.; Antiga, L.; and Lerer, A. 2017. Automatic Differentiation in PyTorch. In *NIPS Autodiff Workshop*.
- Russakovsky, O.; Deng, J.; Su, H.; Krause, J.; Satheesh, S.; Ma, S.; Huang, Z.; Karpathy, A.; Khosla, A.; and Bernstein, M. 2015. ImageNet Large Scale Visual Recognition Challenge. *IJCV*.
- Sakagami, Y.; Watanabe, R.; Aoyama, C.; Matsunaga, S.; Higaki, N.; and Fujimura, K. 2002. The intelligent ASIMO: System overview and integration. In *IEEE/RSJ international conference on intelligent robots and systems*, volume 3, 2478–2483. IEEE.
- Szegedy, C.; Liu, W.; Jia, Y.; Sermanet, P.; Reed, S.; Anguelov, D.; Erhan, D.; Vanhoucke, V.; and Rabinovich, A. 2015. Going Deeper with Convolutions. In *CVPR*.
- Tian, B.; Yao, Q.; Gu, Y.; Wang, K.; and Li, Y. 2011. Video processing techniques for traffic flow monitoring: A survey. In *2011 14th International IEEE Conference on Intelligent Transportation Systems (ITSC)*, 1103–1108. IEEE.
- Vaswani, A.; Shazeer, N.; Parmar, N.; Uszkoreit, J.; Jones, L.; Gomez, A. N.; Kaiser, L.; and Polosukhin, I. 2017. Attention is all you need. In *NIPS*.
- Voigtlaender, P.; Luiten, J.; Torr, P. H. S.; and Leibe, B. 2020. Siam R-CNN: Visual Tracking by Re-Detection. In *CVPR*.
- Wang, Q.; Zhang, L.; Bertinetto, L.; Hu, W.; and Torr, P. H. S. 2019. Fast Online Object Tracking and Segmentation: A Unifying Approach. In *CVPR*.
- Wu, Y.; Lim, J.; and Yang, M. H. 2015. Object Tracking Benchmark. *TPAMI*.
- Yan, B.; Peng, H.; Fu, J.; Wang, D.; and Lu, H. 2021. Learning Spatio-Temporal Transformer for Visual Tracking. In *ICCV*.
- Zhang, Z.; Peng, H.; Fu, J.; Li, B.; and Hu, W. 2020. Ocean: Object-aware Anchor-free Tracking. In *ECCV*.